

U/Pb-dating and geochemical characterization of the Brocken and the Ramberg Pluton, Harz Mountains, Germany

Jana Zech^{1*}, Teresa Jeffries², Dominik Faust³, Bernd Ullrich⁴, Ulf Linnemann⁵

¹ University of Bern, Institute of Geography, Bern, Switzerland
ilgner@giub.unibe.ch

² Natural Historic Science Museum London, London, UK

³ Technische Universität Dresden, Geographisches Institut, Dresden, Germany

⁴ Technische Universität Dresden, Institut für Geotechnik, Dresden, Germany

⁵ Senckenber Naturhistorische Sammlungen Dresden, Museum für Mineralogie und Geologie Dresden
Königsbrücker Landstr. 159, 01109 Dresden, Germany

* Corresponding author

Abstract

The Harz Mountains in Germany form a part of the Variscan basement in the southern part of the Rheno-Hercynian Zone. The area is situated close to the suture between Laurussia and Gondwana represented by the Mid-German Crystalline Zone. The Harz Mountains became intruded by a number of granites that are believed to be related to the Variscan orogeny.

We dated zircons of two samples from the marginal facies of the two major granites Brocken and Ramberg using U/Pb single zircon dating by a Laser-ICP-MS. The measurements of the needle-shaped magmatic zircons show a concordia age of 283 ± 2.1 Ma for the Brocken granite and a concordia age of 283 ± 2.8 Ma for the Ramberg granite. These ages are interpreted as the timing of intrusions, which seem to be related to the opening of the large molasse basins during the Lower Permian and not, as assumed so far, to the Variscan orogeny. The event is characterized by extension and thinning of the crust during the formation of the molasse basins. Geochemical signatures and thin section microscopy support the assumption of a doming in the asthenosphere and a resulting heat flow responsible to the formation of magmas during the Lower Permian.

1. Introduction

The Harz Mountains are situated in the southern part of the Rheno-Hercynian Zone, which are a part of the Central European Variscides. The two major Plutons are the Brocken granite and the Ramberg granite. The orogeny of this massif has been subject of scientific investigations for more than a century, particularly the timing of the intrusion of both granites and the implications for the geotectonic setting and the processes involved. Previous results (Baumann et al. 1991 and references therein) suggest that the intrusion took place postcinematic after the variscian orogeny in the upper Rotliegend. It remains unclear whether the two plutons Brocken and Ramberg intruded cogenetic caused by similar geological origin. According to Feldmann et al. (2002) both granites intruded in the upper lithosphere. This is in agreement with results of Baumann et al. (1991), who dated the intrusion of the Brocken using titanite-isotope analyses to 293–

295 Ma and who assumed the intrusion of the melt in ~ 8 km depth in the lithosphere with temperatures around 300 °C. During the same time period like the Brocken granite the intrusion of the Ramberg granite occurred. Petrographical investigations of Eidam and Seim (1963, 1971, 1974) showed that the core facies of the granite is enriched in plagioclas and depleted in kalifeldspar. Furthermore Eidam and Seim assumed that the Ramberg consists of two different intrusions, which occurred at different times. Tietz (1996) investigated zircons of the granitoid-xenolith of the Bodegang, one of the volcanic lodes in the Harz Mountains. His results show a petrogenetic relation between the Bodegang and the Ramberg concerning the zircon types of the rocks.

In order to contribute to a better understanding of the geological and geotectonic setting of the granite intrusions in the Harz Mountains we (i) applied single zir-

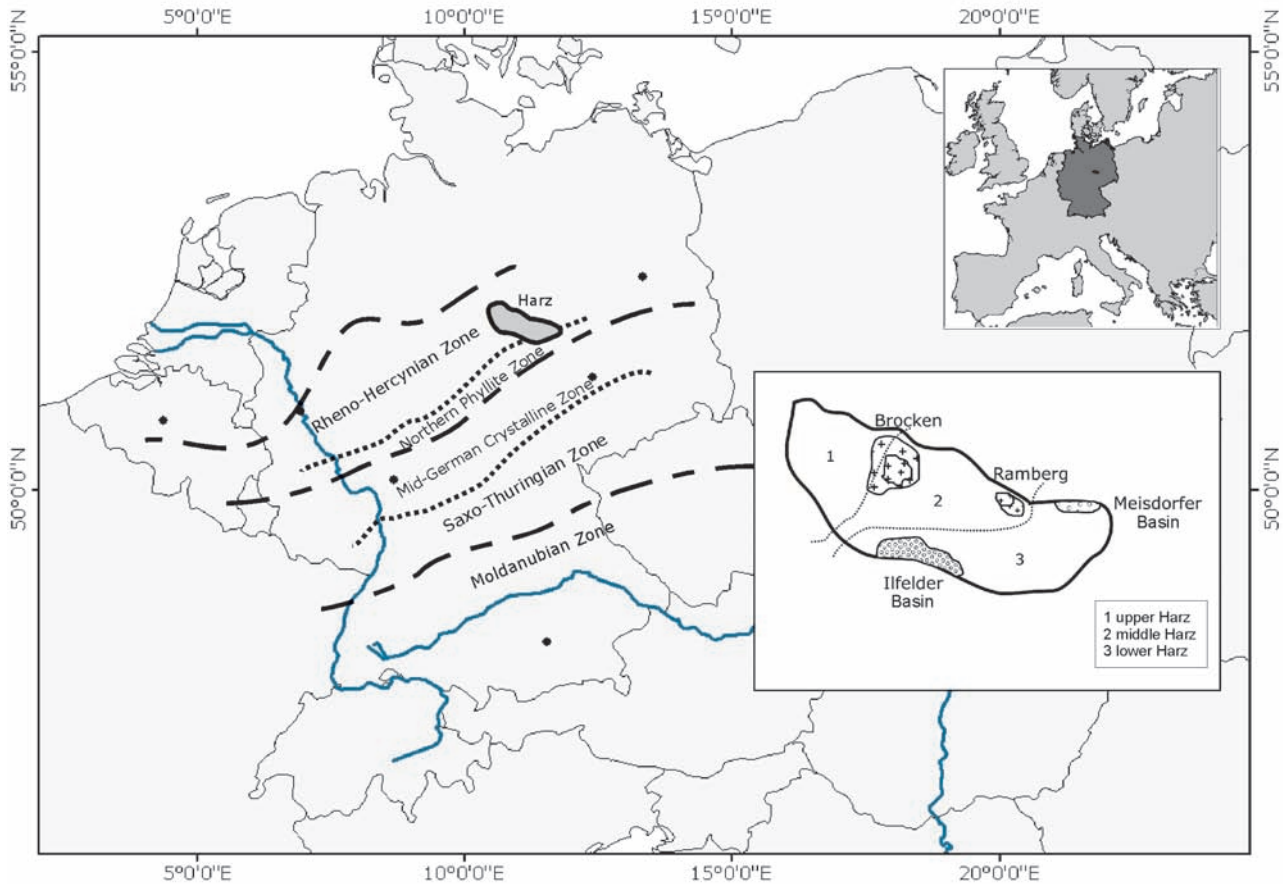


Fig. 1: Geographical setting of the Harz Mountains, Germany.

con U/Pb-istope-dating to the marginal facies of both the Brocken and the Ramberg plutons, which should yield the crystallisation and the intrusion ages, respectively, and (ii) we analysed the geochemical composition and thin sections of samples from core and marginal facies to infer further information about the origin and crystallization of the magmas.

2. Geological setting

The Harz, representing a tectonically uplifted segment, is located in the Rhenohercynian Zone, as one part of the Variscian belt in Central Germany. The Variscian belt can be subdivided into four tectono-stratigraphic segments, which are from NW to SE: the Rhenohercynian

Zone, Mid-German Crystalline Zone, the Saxothuringian Zone and the Moldanubian Zone (Walter 1995). Conglomerations of small crustal blocks characterize the complex of the Variscian belt with different origins along strike-slip and detachment systems. The Harz varies in its geological composition and the magmatic, tectonic, sedimentary and erosional processes that were involved in its genesis. Hence the Harz can be divided from NW to SE in the upper Harz, the middle Harz and the lower Harz (fig. 1). The upper Harz comprises the Oker granite, the Eckergneisscholle, the Harzburger Gabbonorit massive, Diabas and the western part of the Brocken. The middle Harz consists of carboniferic intrusions, Devonian schists, Diabas and greywackes as well as the eastern part of the Brocken granite and the Ramberg granite. Ordovizian and Devonian greywacke formations and molasse basins of the lower Permian form the lower Harz (Mohr 1993). The orogen of the Harz Mountains was caused by the col-

Tab. 1: Geographical coordinates of the sample.

	sample	latitude	longitude
Brocken	bg1 dat	51°47'40.67"	10°32'26.21"
	bg 2	51°48'8.23"	10°32'19.78"
	bg 3	51°51'18.37"	10°32'49.32"
	bg 5	51°46'26.95"	10°40'28.35"
Ramberg	ram 1	51°43'48.20"	11°1'43.66"
	rg 1	51°43'48.56"	11°1'43.44"
	rg 2	51°43'33.29"	11°2'0.39"

lision between Laurussia and Amorika during the Upper Carboniferous, which could be dated based on flysch formations (Wachendorf 2002, and references therein). Due to folding and exhumation and resultant volcanism during the lower Permian (upper Rotliegend) a large number of plutonic rocks crystallized in several stages, and formed cumulus shaped subsurface granites. According to Baumann et al. (1991) the two plutons Brocken and Ramberg intruded into the upper lithosphere between 293–295 Ma. At the same time, such as the Ilfeld basin and the Meisdorf basin developed as a result of the extension of the crust. These molasse basins are filled with up to 800 m of siliciclastics with intercalated vulcaniclastic sediments and lava flows (Feldmann et al. 2002).

3. Sample description

Totally, 15 samples were taken from the marginal facies (fine – middle grained) and from the core facies (porphyry – micropegmatitic grained) of the Brocken and Ramberg granite. The exact co-ordinates of the samples are given in table 1. Samples were free of vegetation and weathering features.

4. Analytical methods

4.1. Single zircon U/Pb-dating

One sample from the marginal facies of the Brocken (sample BG1dat) and one of the Ramberg pluton (sam-

ple RAM 1) was processed for single zircon U/Pb dating. After crushing and sieving to 0.063–2.0 mm, magnetic minerals were removed. The zircons were further purified using a lithium tetraporat density solution. 100–150 undisrupted zircons (30–230 μm) were picked under the microscope and placed into an epoxit resin mount. The U/Pb isotope measurements were conducted at the Natural History Museum London, UK, using a frequency quintupled Nd:YAG based laser ablation system ($\lambda \sim 213 \text{ nm}$) and quadrupole based ICP-MS. Further details concerning the Laser-ICP-MS measurement technique are described in Jeffries et al. (2003). 24 undisrupted zircons from the Brocken Pluton and 46 zircons from the Ramberg Pluton were analysed. Each run of 12 unknowns bracketed by 8 determinations of the standard zircon 91500 (age 1062.5 \pm 1.7Ma) for calibration and mass bias correction. The $^{206}\text{Pb}/^{238}\text{U}$, $^{207}\text{Pb}/^{235}\text{U}$ and $^{207}\text{Pb}/^{206}\text{Pb}$ isotope ratios of the samples and ages are given in table 2 (Brockengranite sample BG1dat) and 3 (Ramberggranite sample RAM1). To obtain the best age estimate the $^{206}\text{Pb}/^{238}\text{U}$ and the $^{207}\text{Pb}/^{235}\text{U}$ isotope ratios were correlated (Ludwig, 1998). Only the concordant isotope ratios that overlap the concordia with a 2σ error ellipse were used to determine the concordia age. Ages and errors were calculated by using the Isoplot software of Ludwig (2001). The decay constants by the IUGS (Steiger and Jäger 1977) were applied.

4.2. Geochemistry and thin sections

Seven samples from both plutons were analyzed concerning the geochemical composition and the thin sections in order to characterize the lithology of the granites. Important parameters to distinguish different granite types are major element ratios, like $\text{Al}_2\text{O}_3 / \text{SiO}_2$ or $\text{Na}_2\text{O} + \text{K}_2\text{O} / \text{SiO}_2$. This reflects mainly the quartz enrichment and the alkali concentration (Linnemann and Romer 2002). The ASI according to Shand (1947: $\text{Al}_2\text{O}_3 / (\text{CaO} + \text{Na}_2\text{O} + \text{K}_2\text{O})$ reflects the Al saturation degree (Markl 2004). $\text{K}_2\text{O}/\text{Na}_2\text{O}$ reflects the content of K-feldspar and mica relative to the plagioclase (Linnemann and Romer 2002). To characterize the chemical weathering, especially for feldspar and therefore the ratio of mobile elements to immobil ones Al_2O_3 vs. $(\text{CaO} + \text{Na}_2\text{O})$ is decisive. The correlation of the trace elements and REE, e.g. Rb vs. Y + Nb is used to determine the geological setting (Pearce et al. 1984).

Major, trace and rare earth elements (REE) were determined by ACTLABS (Ancaster, Ontario, Canada) us-

ing lithium metaborate/tetraborate fusion and Inductive Coupled Plasma Mass Spectroscopy (ICP-MS). Quality tests for the measurements are available through reference materials with known geochemical composition. The geochemical composition and the detection limits of all samples are given in table 4. For data analysis and interpretation of the geochemical signatures the program minpet version 2.02 was used.

4.3. Scanning electron microscopy

Morphology of single zircon crystals, the fabric of thin sections and the chemical composition of single feldspar crystals were investigated by means of scanning electron microscope (SEM) ZEISS EVO 50 coupled with an energy dispersive micro analytical spectrometer (EDS) ROENTEC detector XFlash 3001 (Quantax 1.7.) and a cathodoluminescence detector (CL) SEM-CL-view (EMSystems).

5. Results and discussion

5.1. Single zircon U/Pb-dating

Six out of 24 zircons of BG1dat yielded mixed ages for the $^{206}\text{Pb}/^{238}\text{U}$, $^{207}\text{Pb}/^{235}\text{U}$ and $^{207}\text{Pb}/^{206}\text{Pb}$ isotope ratios (table 2) indicating recrystallization and/or alteration and were therefore excluded from age calculations. Concerning the Ramberg granite eight out of 46 zircons were excluded likewise because of mixed ages (table 3). The concordia-ages (fig. 2 and 3) calculated for the remaining zircons are 283.0 ± 2.1 Ma (BG1dat) and 283.0 ± 2.8 Ma (RAM1), respectively. These ages are interpreted to reflect the timing of the crystallization of both granites. A second concordia-age for the Ramberg is 289.3 ± 0.59 Ma. This is likely due to crystallisation of magma resulting from another, previous intrusion. The shape of the zircons from both Plutons is, however, very similar and can be divided into three subpopulations: i) needle shaped ii) lath prismatic and iii) thick prismatic (fig. 4). Reasons for that are i) the spatial nearness, ii) the similar geological conditions during crystallization and iii) a cogenetic formation through the same geotectonical strength. Within this classification the dated crystallization ages of all zircons vary over the total age range. The zircons of BG1dat can be characterized

as D, P5 and S25 – idiomorphic, needle-shaped crystals following the zircon classification scheme of Pupin and Turco (1972). Additionally no inherited cores existed. The zircons have been formed by a magmatic early crystallization by temperatures of 800–900 °C. Those conditions in the lithosphere suggest a doming of the asthenosphere and a contamination of the meltings by an intruding fluidal phase out of the asthenosphere. The zircons of the population RAM1 are mainly G1 and P1 types following Pupin and Turco (1972) and featured traces of alteration. These shapes have been formed under temperature conditions between 600–650 °C, which reflect the crystallization in the upper lithosphere.

5.2. Geochemistry

The geochemical results are shown in table 4 and fig. 8 and 9. The concentrations of some elements, especially for several trace elements are lower than the detection limit. Brocken and Ramberg samples can be characterized as felsic A-type granites. According to the granite characterization of Pearce et al. (1984) the samples of the Brocken Pluton (BG1dat, BG2, BG3, BG5) refer to within-plate granites (WPG), more specifically granites in attenuated continental crust. The samples RAM1 and RG5 of the Ramberg Pluton are posttectonically crystallized collisional granites (syn-COLG) enriched in Rb and depleted in Y and Nb. The sample RG1 can be classified as volcanic-arc granite (VAG) indicating crystallization in spheres of attenuated continental crust.

Considering the element composition within the single granite complexes the concentration becomes lesser from the core to the marginal facies. The ASI after Shand shows that all samples of both granite massifs are peraluminous. Although the two plutons are spatial near, element compositions and concentration vary widely. The major elements, REE and trace elements are significant enriched in the Brocken granite. To specify the determined concentration of the elements are up to three times higher than the measured ones of the Ramberg granite, excluding P_2O_5 and MgO. Both plutons have a decrease of REE and a specific negative Eu anomaly in common. Typically for a-type granites are the low ratios of $\text{K}_2\text{O}/\text{Na}_2\text{O}$ (3.43–1.72) and a variable SiO_2 concentration between 73.34 % and 82.93 %. All samples are characterized by an enrichment of Al_2O_3 , especially the Brocken granite samples: $\text{Al}_2\text{O}_3 > 11.62$ %. This concentration decreases

Tab. 2: $^{206}\text{Pb}/^{238}\text{U}$, $^{207}\text{Pb}/^{235}\text{U}$ and $^{207}\text{Pb}/^{206}\text{Pb}$ isotope ratios and ages of the Brocken granite samples.

Sample	$^{208}\text{Pb}/^{206}\text{Pb}$	$^{206}\text{Pb}/^{238}\text{U}$	$^{207}\text{Pb}/^{235}\text{U}$	$^{207}\text{Pb}/^{206}\text{Pb}$	$^{208}\text{Pb}/^{232}\text{Th}$	$^{206}\text{Pb}/^{238}\text{U}$	$^{207}\text{Pb}/^{235}\text{U}$	$^{207}\text{Pb}/^{206}\text{Pb}$	$^{207}\text{Pb}/^{235}\text{U}$	$^{207}\text{Pb}/^{206}\text{Pb}$	$^{208}\text{Pb}/^{232}\text{Th}$	$^{208}\text{Pb}/^{232}\text{Th}$	
BG 1 dat	ratio	ratio	ratio	ratio	ratio	Age (Ma)	Age (Ma)	Age (Ma)	Age (Ma)	Age (Ma)	Age (Ma)	Age (Ma)	
						$\pm 2s$	$\pm 2s$	$\pm 2s$	$\pm 2s$	$\pm 2s$	$\pm 2s$	$\pm 2s$	
BG 1	0,2637	0,0452	0,3239	0,05201	0,01166	285	2	285	5	284	48	234	3
BG 2	0,227	0,0443	0,3142	0,05146	0,01185	279	3	277	8	260	80	238	6
BG 3	0,2614	0,0436	0,3217	0,05344	0,012	275	6	283	6	346	96	241	7
BG 4 (mixed age)	0,3085	0,0505	0,7906	0,11346	0,02743	318	11	592	47	1854	130	547	41
BG 5	0,219	0,0463	0,3438	0,05388	0,01339	292	3	300	3	364	26	269	5
BG 6	0,1915	0,047	0,339	0,05233	0,01363	296	2	296	3	298	26	274	4
BG 7	0,1927	0,047	0,3616	0,05582	0,01401	296	4	313	8	444	44	281	7
BG 8 (mixed age)	0,222	0,0464	0,4094	0,06395	0,01643	292	4	348	22	740	142	329	18
BG 9	0,2131	0,0446	0,3181	0,0517	0,01346	281	3	280	6	272	62	270	5
BG 10 (mixed age)	0,2308	0,0474	0,4497	0,06882	0,01717	298	4	377	23	892	134	344	18
BG 11 (mixed age)	0,1296	0,0467	0,4673	0,07255	0,02399	294	7	389	28	1000	130	479	51
BG 12	0,2929	0,0429	0,3506	0,05921	0,01352	271	6	305	15	574	132	272	4
BG 13 (mixed age)	0,2393	0,0442	0,3857	0,0633	0,01318	279	3	331	23	718	162	265	9
BG 14	0,2223	0,0438	0,3325	0,05503	0,01281	276	3	292	5	412	48	257	5
BG 15	0,1314	0,0474	0,3496	0,0535	0,01264	298	4	304	5	350	38	254	4
BG 16	0,2668	0,0464	0,3973	0,06204	0,01418	293	4	340	7	674	52	285	5
BG 17	0,1589	0,0437	0,3155	0,05235	0,01193	276	5	278	5	300	62	240	8
BG 18	0,265	0,0463	0,3414	0,0535	0,01304	292	2	298	4	350	38	262	3
BG 19	0,216	0,0448	0,3306	0,05346	0,01276	283	3	290	6	348	62	256	8
BG 20	0,2437	0,0458	0,3555	0,05624	0,01328	289	2	309	7	460	54	267	5
BG 21	0,2524	0,0454	0,3284	0,05249	0,01297	286	4	288	5	306	56	260	6
BG 22	0,1628	0,0451	0,3342	0,05372	0,01316	284	3	293	5	358	52	264	7
BG 23 (mixed age)	0,4106	0,0579	1,4026	0,17557	0,0401	363	11	890	41	2610	88	795	43
BG 24	0,2184	0,0448	0,3228	0,05225	0,01276	282	3	284	4	296	54	256	6

Tab. 3: $^{206}\text{Pb}/^{238}\text{U}$, $^{207}\text{Pb}/^{235}\text{U}$ and $^{207}\text{Pb}/^{206}\text{Pb}$ isotope ratios and ages of the Ramberg granite samples.

Sample	$^{208}\text{Pb}/^{206}\text{Pb}$ ratio	$^{206}\text{Pb}/^{238}\text{U}$ ratio	$^{207}\text{Pb}/^{235}\text{U}$ ratio	$^{207}\text{Pb}/^{206}\text{Pb}$ ratio	$^{208}\text{Pb}/^{232}\text{Th}$ ratio	$^{206}\text{Pb}/^{238}\text{U}$ Age (Ma)	$\pm 2s$	$^{207}\text{Pb}/^{235}\text{U}$ Age (Ma)	$\pm 2\sigma$	$^{207}\text{Pb}/^{206}\text{Pb}$ Age (Ma)	$\pm 2\sigma$	$^{208}\text{Pb}/^{232}\text{Th}$ Age (Ma)	$\pm 2\sigma$
RAM 1	0,1068	0,0424	0,3058	0,05228	0,01132	268	6	271	7	296	88	227	7
RAM 2	0,1336	0,044	0,327	0,05387	0,01179	278	4	287	7	364	72	237	9
RAM 3	0,1651	0,0437	0,3175	0,05268	0,01108	276	4	280	5	314	48	223	9
RAM 4	0,0976	0,0449	0,3296	0,05324	0,01143	283	3	289	7	338	58	230	7
RAM 5	0,1287	0,0434	0,3202	0,05344	0,01141	274	4	282	12	346	102	229	11
RAM 6	0,0502	0,0481	0,3438	0,05186	0,01117	303	5	300	9	278	86	225	9
RAM 7	0,1688	0,0444	0,3158	0,05153	0,01173	280	7	279	8	264	74	236	9
RAM 8	0,1944	0,0451	0,3297	0,05301	0,01172	284	4	289	4	328	36	235	7
RAM 9	0,1588	0,0453	0,3376	0,05399	0,01167	286	4	295	9	370	92	235	6
RAM 10	0,1752	0,0448	0,3355	0,05431	0,01149	283	5	294	7	384	68	231	9
RAM 11	0,2539	0,0436	0,3048	0,05069	0,01174	275	3	270	7	226	70	236	5
RAM 12	0,16	0,0444	0,3309	0,05408	0,0113	280	4	290	7	374	56	227	6
RAM 13	0,1434	0,044	0,4082	0,06723	0,00796	278	6	348	15	844	82	160	7
RAM 14	0,1032	0,045	0,318	0,0513	0,01083	283	5	280	8	254	78	218	8
RAM 15	0,0906	0,0448	0,3305	0,05352	0,01029	282	3	290	6	350	48	207	8
RAM 16	0,1747	0,0453	0,3222	0,05162	0,01053	285	6	284	8	268	86	212	9
RAM 17	0,0772	0,0453	0,3288	0,05265	0,01065	285	3	289	4	312	36	214	6
RAM 18	0,158	0,0458	0,3384	0,05352	0,01023	289	3	296	4	350	40	206	4
RAM 19	0,0824	0,0446	0,3274	0,0532	0,01053	281	2	288	5	336	48	212	4
RAM 20	0,0697	0,0441	0,3218	0,05296	0,01071	278	6	283	7	326	80	215	10
RAM 21	0,1154	0,0455	0,3259	0,05198	0,01055	287	4	286	5	284	42	212	5
RAM 22	0,1237	0,0468	0,3503	0,05427	0,00983	295	4	305	6	382	48	198	5
RAM 23 (mixed age)	0,3283	0,1208	1,3916	0,08355	0,03434	735	59	885	71	1282	110	683	25
RAM 24 (mixed age)	0,0533	0,2534	3,7433	0,10714	0,05995	1456	54	1581	36	1750	16	1177	41
RAM 25	0,0993	0,0465	0,3523	0,05493	0,01154	293	7	306	8	408	96	232	9

Tab. 3: Continuation.

RAM 26	0,045	0,0441	0,3268	0,0537	0,01	278	4	287	12	356	124	232	10
RAM 27	0,09	0,0460	0,3297	0,0520	0,01	290	4	289	9	284	84	225	9
RAM 28	0,1206	0,0450	0,3314	0,0534	0,01	284	4	291	6	346	52	214	6
RAM 29	0,148	0,0453	0,3254	0,0521	0,01	286	6	286	9	288	92	215	6
RAM 30 (mixed age)	0,1524	0,0628	0,4909	0,0567	0,01	393	9	406	13	476	68	290	7
RAM 31	0,1653	0,0453	0,3648	0,0584	0,01	286	4	316	9	544	70	245	8
RAM 32 (mixed age)	0,1218	0,0616	0,5159	0,0608	0,02	385	25	422	34	630	76	355	25
RAM 33	0,1261	0,0456	0,3340	0,0531	0,01	288	3	293	7	330	64	222	8
RAM 34	0,1788	0,0460	0,3294	0,0519	0,01	290	4	289	9	280	96	223	6
RAM 35	0,0485	0,0454	0,3292	0,0526	0,01	286	4	289	7	312	62	232	11
RAM 36 (mixed age)	0,1652	0,0463	0,3537	0,0537	0,01167	292	6	308	7	426	84	234	9
RAM 37	0,1562	0,061	0,4595	0,05464	0,01464	382	7	384	7	396	58	294	11
RAM 38	0,1365	0,1563	1,592	0,07384	0,03436	936	24	967	16	1036	36	683	25
RAM 39	0,163	0,0463	0,336	0,05262	0,01078	292	5	294	9	312	90	217	7
RAM 40	0,0712	0,0439	0,3226	0,05324	0,01146	277	4	284	9	338	84	230	13
RAM 41	0,1313	0,0464	0,3332	0,05204	0,011	293	6	292	13	286	106	221	9
RAM 42	0,1724	0,0462	0,3339	0,05244	0,01101	291	3	293	5	304	46	221	5
RAM 43	0,1235	0,047	0,3465	0,0535	0,01125	296	4	302	9	348	78	226	11
RAM 44 (mixed age)	0,0425	0,047	0,491	0,07579	0,01391	296	45	406	49	1088	40	279	15
RAM 45	0,1153	0,0489	0,3724	0,0552	0,01174	308	5	321	9	420	86	236	10
RAM 48	0,1081	0,0454	0,3324	0,05312	0,01159	286	4	291	6	332	64	233	9

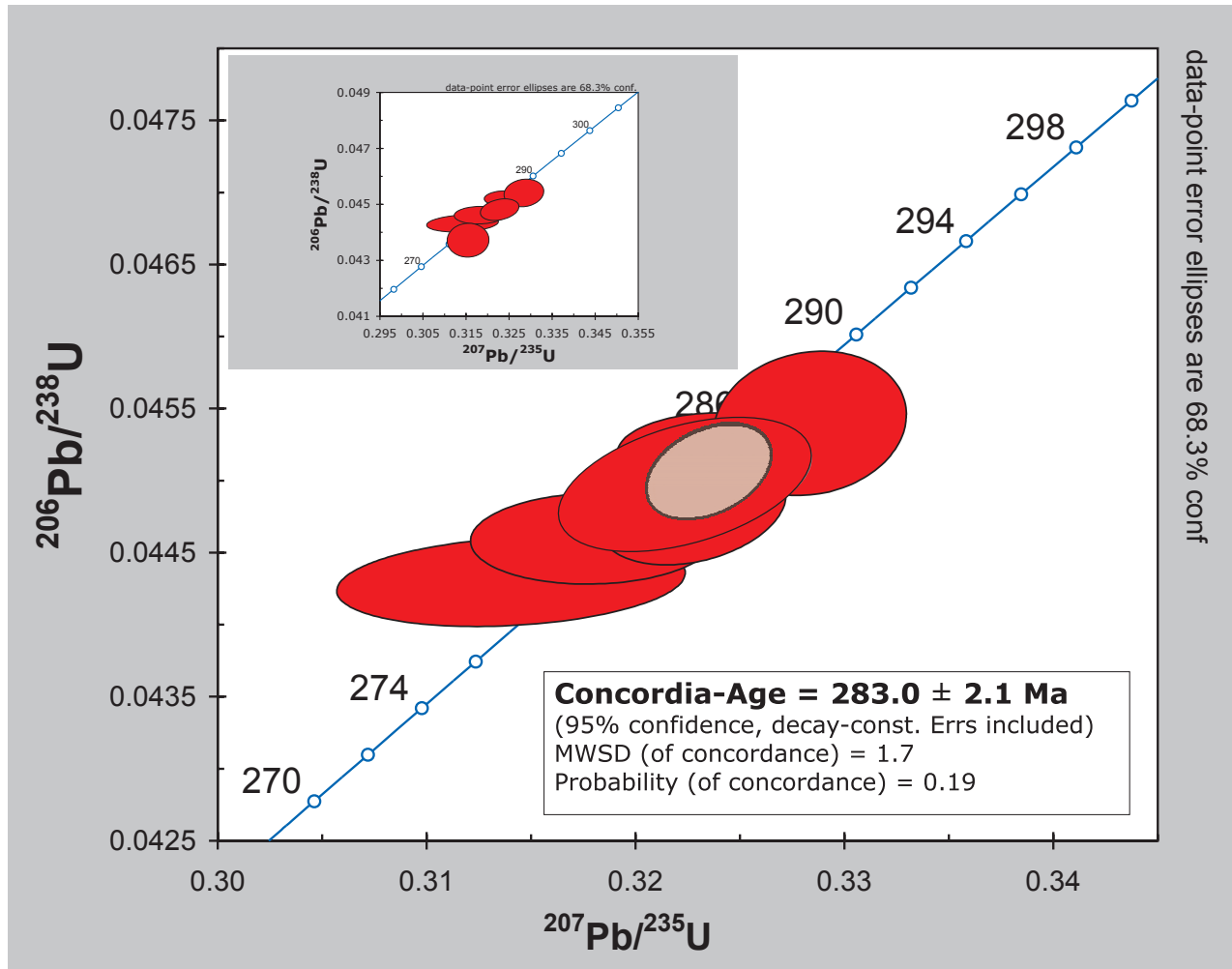


Fig. 2: Concordia-diagram of the Brocken granite sample BG1dat.

es from the core (BG5: 13.15 %) to the marginal facies (BG1dat: 11.62 %). Additionally, the depletion of Na_2O is more marked in the Ramberg samples and follows also a depletion gradient from the core (RG1: 5.12 %) to the marginal facies (RAM1: 1.58 %). Typical for upper lithospheric rocks the Ramberg granite is enriched in SiO_2 . The different distribution of the major elements of the samples leads to the conclusion that inspite of the spatial nearness these plutons intruded and crystallized in different regions and different geochemical milieus of the lithosphere. The granitic melt, which formed the Ramberg intruded in the upper lithosphere. The Ramberg granite exhibit a typical lithospheric element composition with enrichment in light metals, trace elements, like K, Cs Ba and SiO_2 . The elements Na, K, Ca are depleted. This result could be sup-

ported by the thin sections in which no plagioclase could be found in the marginal facies samples and by the slightly shattered zircons. Our results are in good agreement with Eidam and Seim (1971), who noticed a higher concentration of kalifeldspar then plagioclas in the core facies of the Ramberg granite. The sample RG1 of the Ramberg granite has significantly different geochemical results for all analysed elements ($\text{SiO}_2 = 82.93\%$, $\text{Na}_2\text{O} = 5.12\%$, Ba = 10 ppm, Rb = 2 ppm, La = 2,6 ppm, Ce = 6,4 ppm, Nd = 5,0 ppm, Eu = 0,16 ppm, U = 1,4 ppm). Because there is only one sample we are hesitant to interpret this result. One possible explanation could be that this sample refers to a geochemical zonation in the core facies. The geological setting of the Brocken granite took place in the lower crust in contamination to the doming asthe-

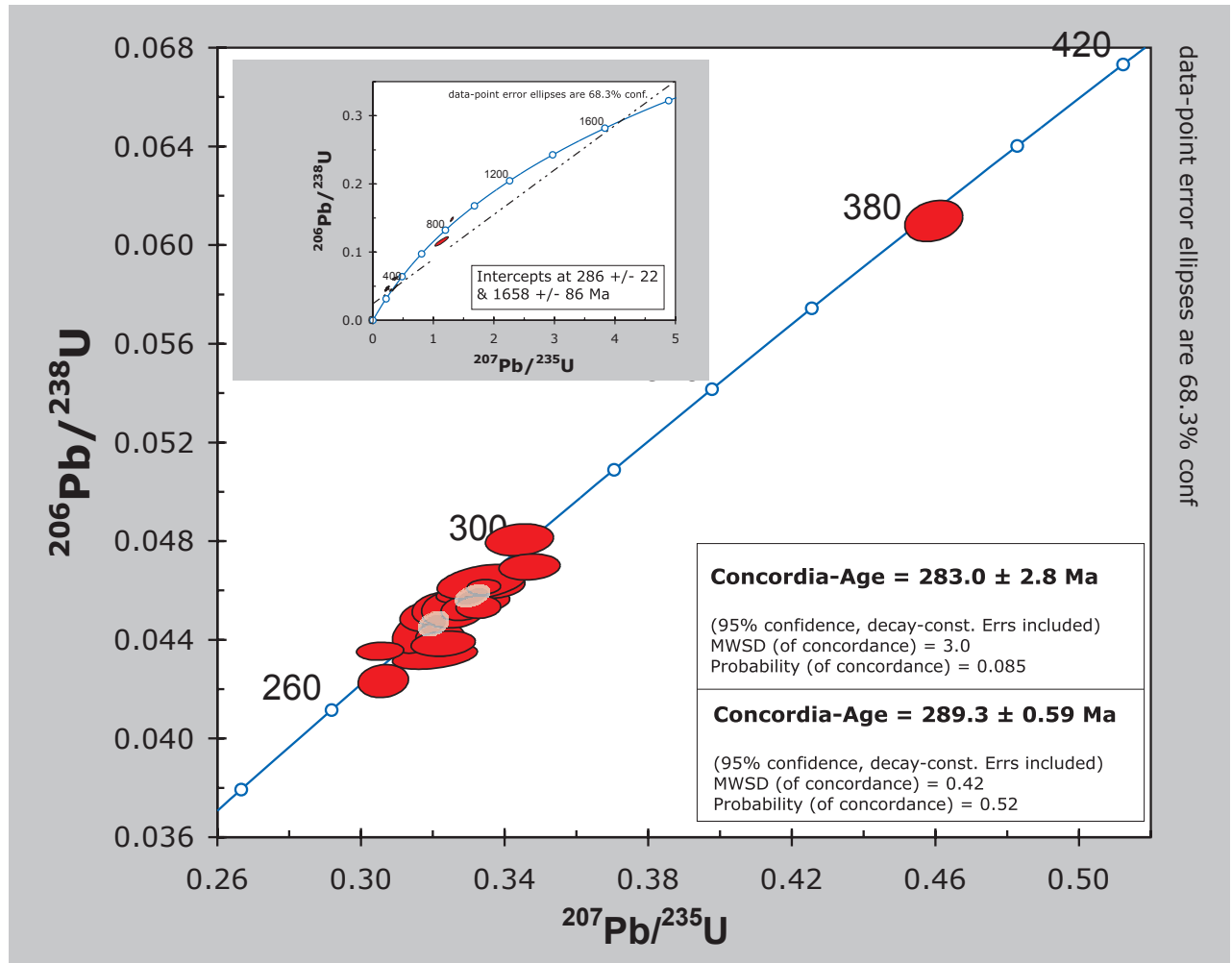


Fig. 3: Concordia-diagram of the Ramberg granite sample RAM1.

nosphere resulting from the extension and thinning of the crust during the formation of the molasse basins. The enrichment in asthenospheric elements in the Brocken granite samples leads to the assumption that a resulting heat flow intruded in the lower lithosphere. This led to a variety composition of lithospheric and asthenospheric elements in the Brocken granite in accordance to an primitive mantle rock with a high concentration of heavy metals, especially of the elements Rb, Nb, Zr and Ti and REE. In addition this intrusion caused depletion of Eu and of the volatile elements Na, K, Ca, which explains the negative Eu anomaly of all granitic samples. Furthermore the melt of the rocks were once crystallized and then melted again before recrystallization. In a primary melt the plagioclases were partial melted through anatexis. The mobil

elements reacted volatile and a depletion of the cations Na, K, Ca and Eu as well as an enrichment of Al were caused. The melt of the Ramberg intruded in phases so that the already crystallized plagioclases were fractionated by the intruding fluidal phase out of the asthenosphere. Moreover, the educts of both melts could already have a negative Eu anomaly and the feldspar existed only subordinate.

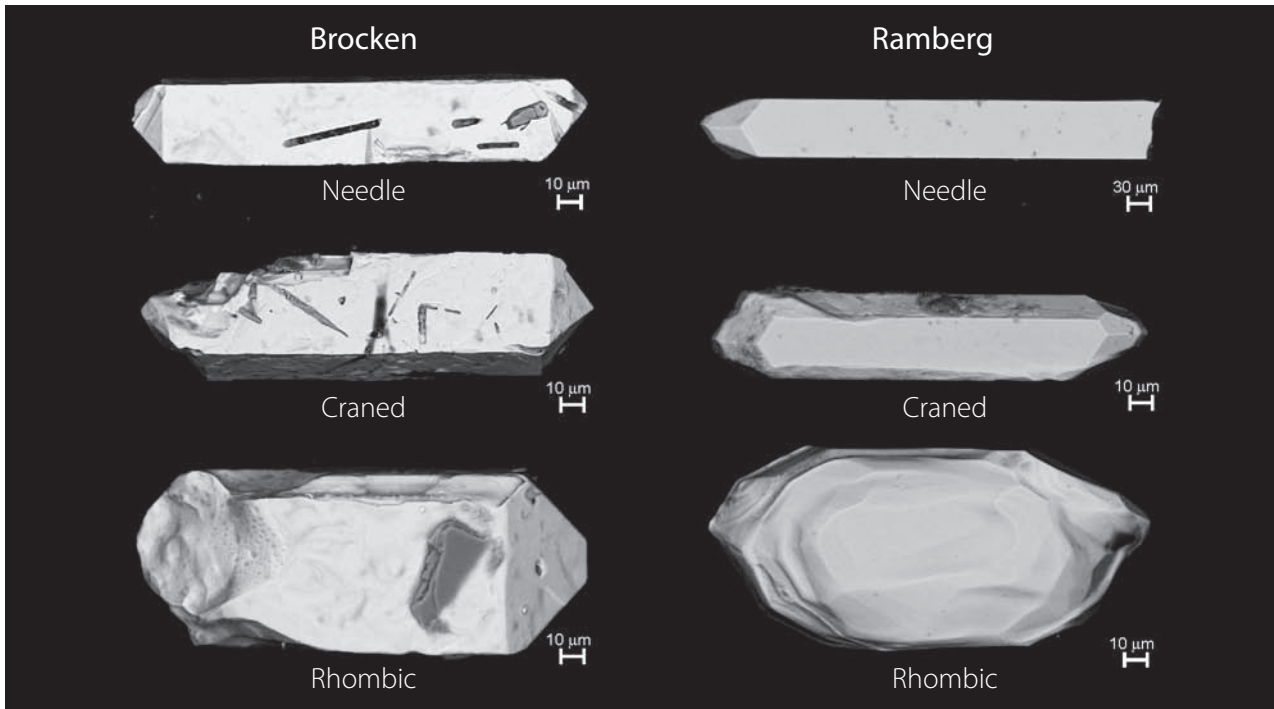


Fig. 4: 3-D microscopic photographs of zircons from Brocken and Ramberg, Harz, Germany. The habitus description of the zircons is below the microphotograph.

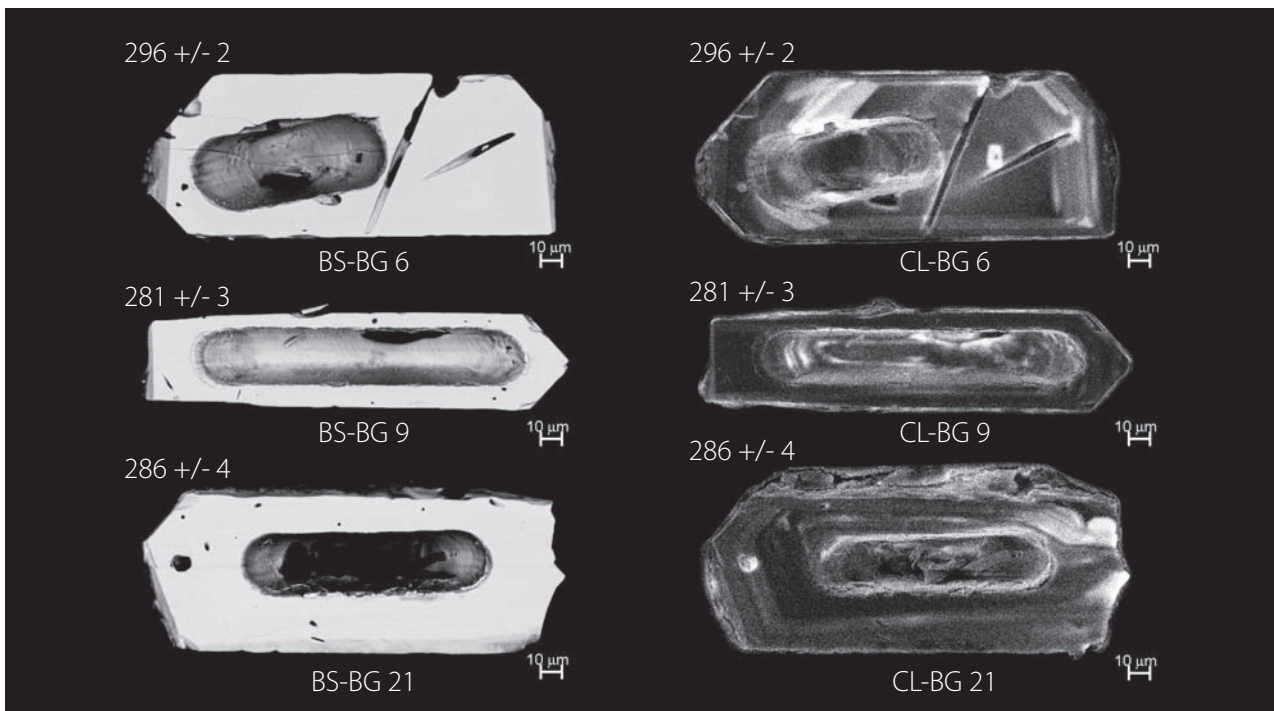


Fig. 5: Electron microscopic photographs of the zircons BG 6, BG 9 and BG 21 from the Brocken granite sample. Zircon ages are in Ma. BS – back scatter, CL–ca thodoluminescence.

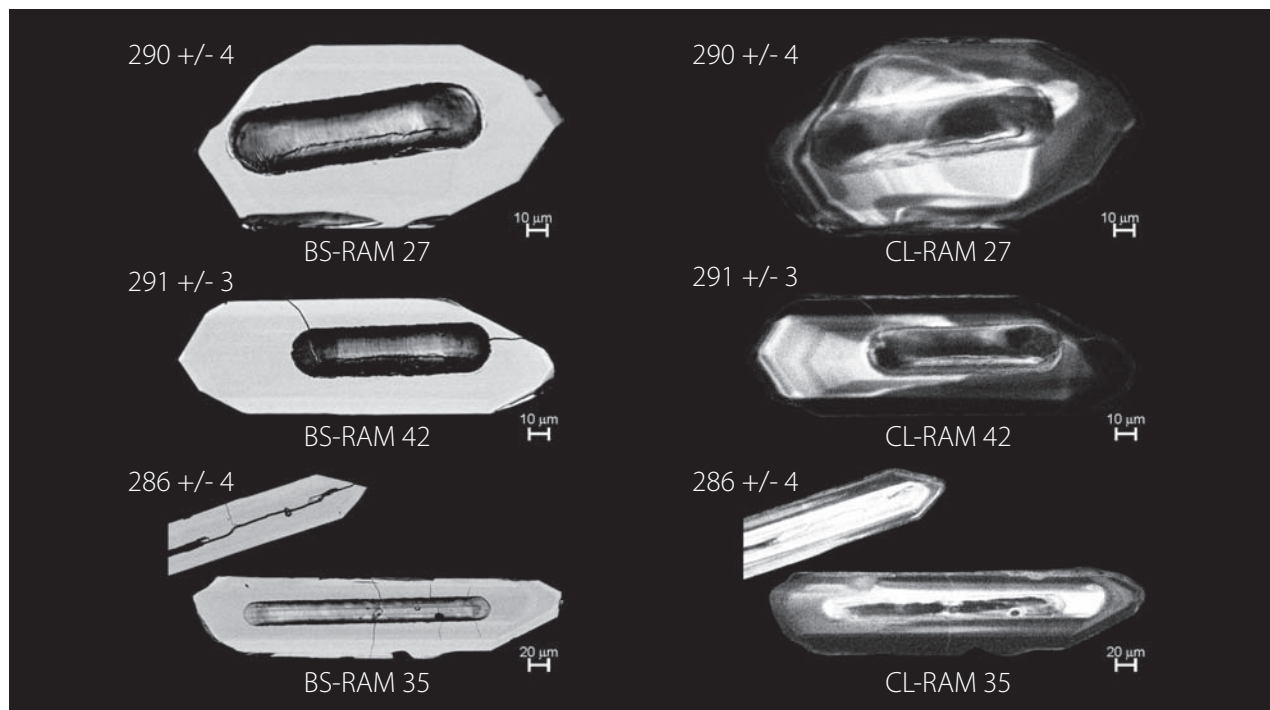


Fig. 6: Electron microscopic photographs of the zircons RAM 27, RAM 42 and RAM 35 from the Ramberg granite sample. Zircon ages are in Ma. **BS** – back scatter, **CL** – cathode-luminescence.

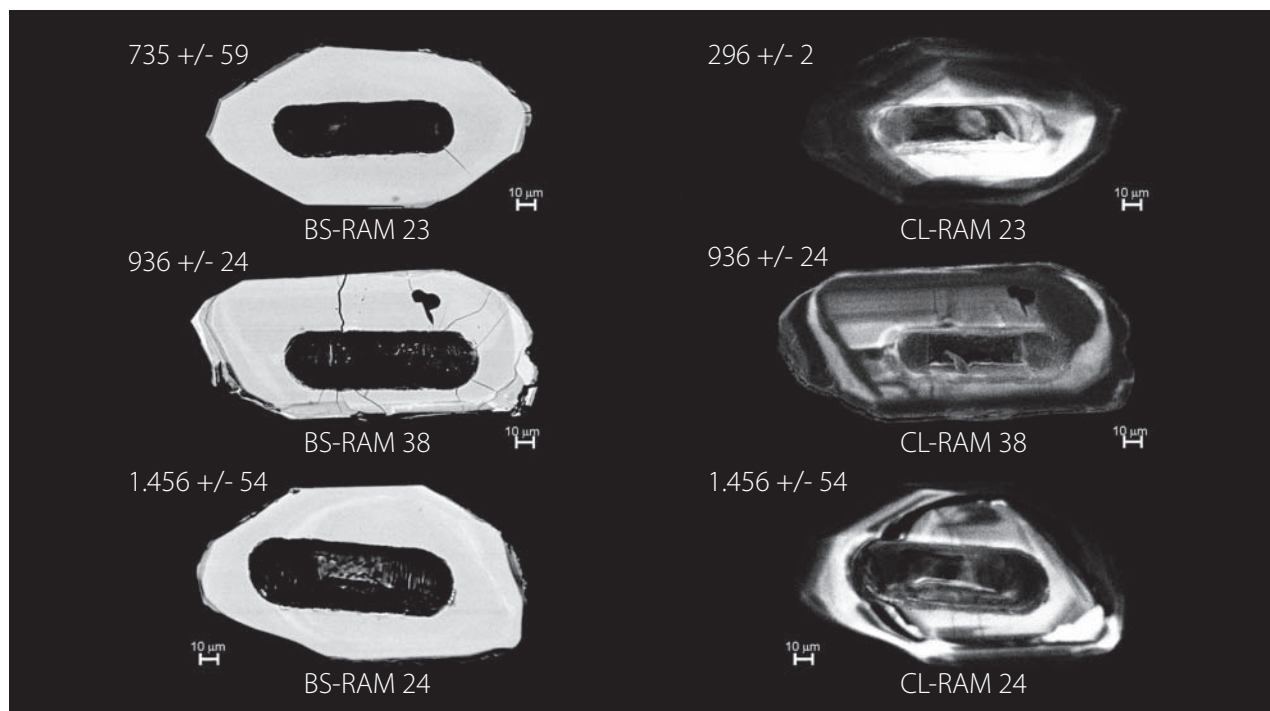


Fig. 7: Electron microscopic photographs of zircons RAM 23, RAM 38 and RAM 24 from the Ramberg granite sample. Zircon ages are in Ma. **BS** – back scatter, **CL** – cathodoluminescence.

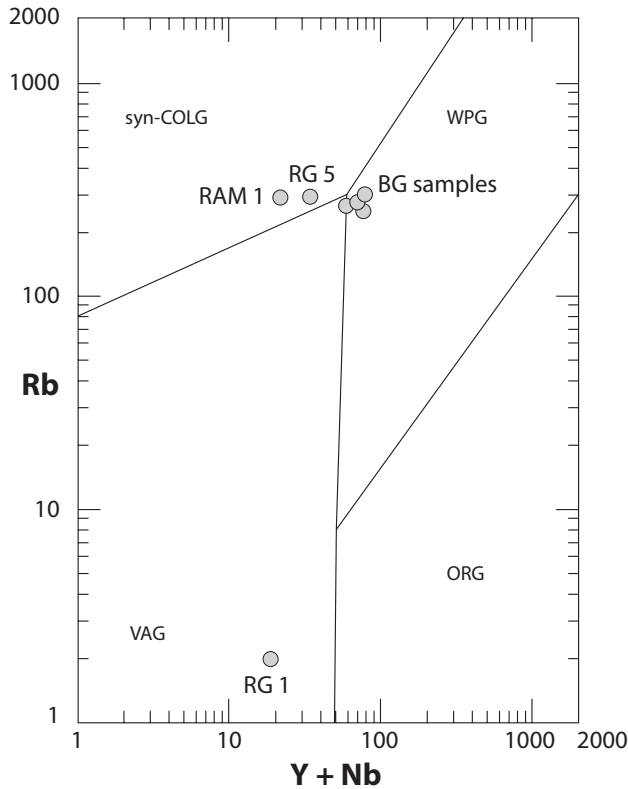


Fig. 8: Rb vs. Y+Nb discrimination diagram after Pearce et al. (1989). **BG** – Brocken granite samples RAM, **RG** – Ramberg granite samples.

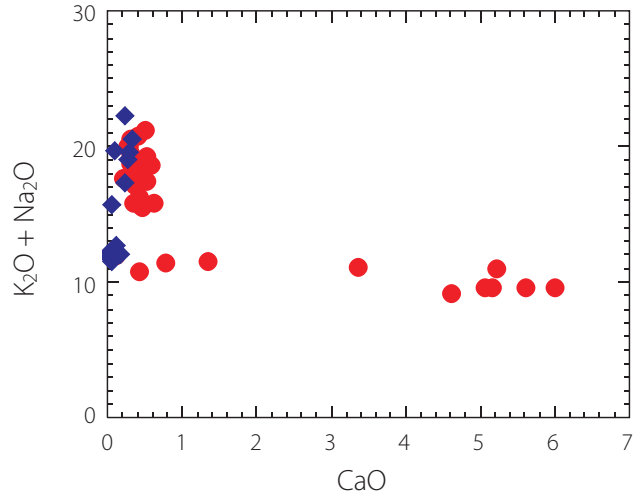
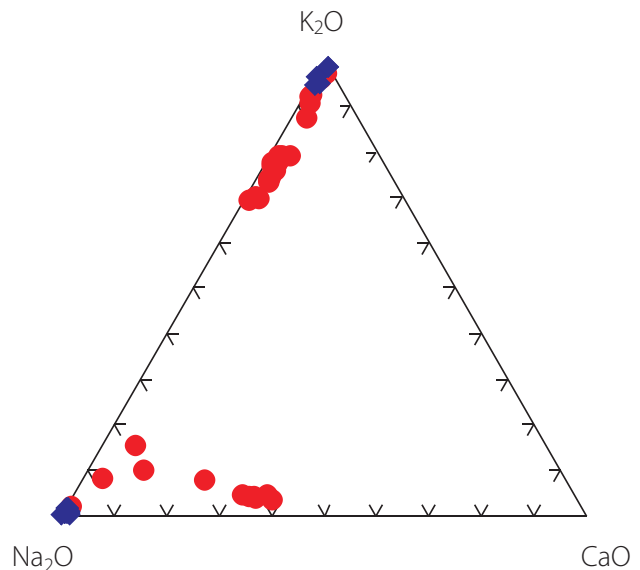


Fig. 9: Concentration of the feldspar oxides Na₂O, K₂O and CaO. **Red** – Brocken granite samples. **Blue** – Ramberg granite samples.



5.3. Thin sections

The previous results are supported by thin section analyses. The analysed samples, excluding RG1, refer to the rock classification granite. The marginal facies of the Ramberg Pluton (sample RG1) belongs to alkali feldspar granite. The Ramberg granite samples are inherent in micrographic growing between the kalifeldspars and the quartz minerals as it is typical for intrusions in the upper lithosphere. The hypidiomorphic plagioclases are often characterized by twin formations. Only in the core facies of the Ramberg (samples RAM1, RG5) both feldspars could be identified. The Brocken granites are char-

acterized by myrmecitic growings between plagioclase and kalifeldspar (fig. 10 top: kalifeldspar and quartz, bottom: plagioclase, kalifeldspar and quartz). This demonstrates the contamination of the crystallizing melt with the fluidal mantle magma. The enrichment of feldspar and mica are in accordance with the concentration of the mineral forming elements of the geochemical signature. The dominance of kalifeldspar reflects the depletion of Na₂O + CaO / K₂O. In the core facies (RG1) the dominance of plagioclase is in agreement with the high concentration of Na₂O + CaO / K₂O of the geochemical analyses. The kalifeldspars showed kaolinization and the plagioclases sericitization feature.

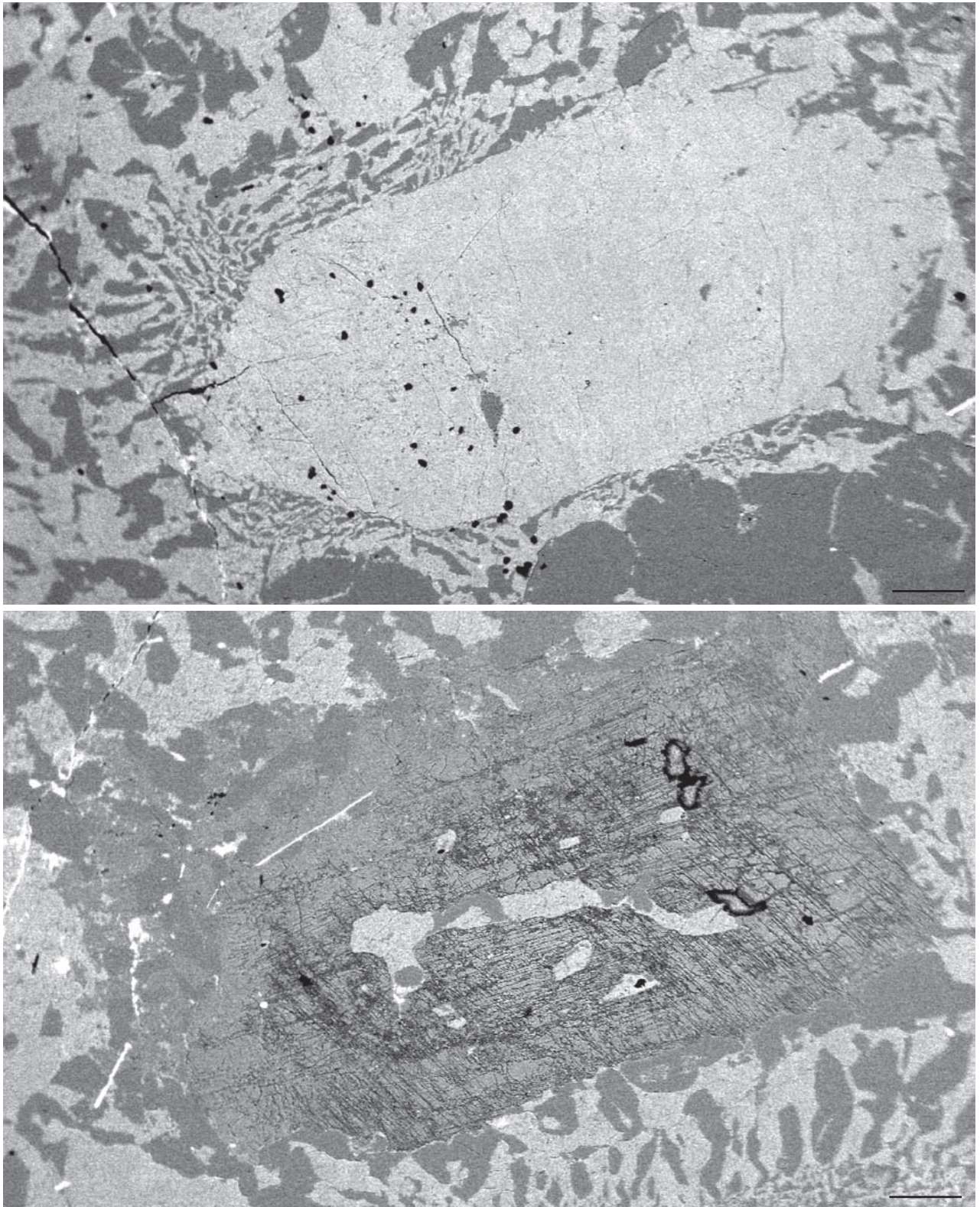


Fig. 10: The typical myrmecitic texture of the Brocken granite samples, documented by the thin section of sample BG 2. Scale = 200 μm .

Tab. 4: Geochemical results of the Brocken granite and Ramberg granite samples.

Element:	SiO ₂	Al ₂ O ₃	Fe ₂ O ₃ (T)	MnO	MgO	CaO	Na ₂ O	K ₂ O	TiO ₂	P ₂ O ₅	LOI	Total	Sc	Be	V	Ba	Sr	Y	Zr
Units:	%	%	%	%	%	%	%	%	%	%	%	%	ppm	ppm	ppm	ppm	ppm	ppm	ppm
Detection Limit:	0.01	0.01	0.01	0.001	0.01	0.01	0.01	0.01	0.001	0.01	0.01	0.01	1	1	5	3	2	2	4
Reference Method:	FUS-ICP	FUS-ICP	FUS-ICP	FUS-ICP	FUS-ICP	FUS-ICP	FUS-ICP	FUS-ICP	FUS-ICP	FUS-ICP	FUS-ICP	FUS-ICP	FUS-ICP	FUS-ICP	FUS-ICP	FUS-ICP	FUS-ICP	FUS-ICP	FUS-ICP
Client I.D.																			
RAM 1	78.35	11.04	1.88	0.021	0.17	0.19	1.58	5.43	0.094	0.09	1.09	99.93	3	<1	<5	184	31	14	49
RG 1	82.93	9.36	1.43	0.012	0.11	0.26	5.12	<0.01	0.081	0.1	0.36	99.77	<1	2	<5	10	49	14	43
RG 5	74.83	12.85	2.23	0.031	0.2	0.34	2.43	5.36	0.114	0.15	1.05	99.58	4	2	5	168	36	21	64
BG 1D	75.9	11.62	2.2	0.047	0.06	0.57	2.9	4.99	0.154	0.03	0.78	99.27	5	3	17	514	37	38	194
BG 3	75.37	12.29	2.45	0.038	0.13	0.29	2.78	5.31	0.187	0.05	1.08	99.97	6	2	<5	344	57	54	196
BG 5	73.34	13.15	2.64	0.036	0.2	1	2.88	5.37	0.222	0.07	0.76	99.68	7	3	7	530	82	55	239
BG 2	75.87	12.26	2.14	0.033	0.09	0.24	2.76	5.68	0.16	0.02	0.73	99.97	6	2	<5	535	50	53	218
Element:	Cr	Co	Ni	Cu	Zn	Ga	Ge	As	Rb	Nb	Mo	Ag	In	Sn	Sb	Cs	La	Ce	Pr
Units:	ppm	ppm	ppm	ppm	ppm	ppm	ppm	ppm	ppm	ppm	ppm	ppm	ppm	ppm	ppm	ppm	ppm	ppm	ppm
Detection Limit:	20	1	20	10	30	1	1	5	2	1	2	0.5	0.2	1	0.5	0.5	0.1	0.1	0.05
Reference Method:	FUS-MS	FUS-MS	FUS-MS	FUS-MS	FUS-MS	FUS-MS	FUS-MS	FUS-MS	FUS-MS	FUS-MS	FUS-MS	FUS-MS	FUS-MS	FUS-MS	FUS-MS	FUS-MS	FUS-MS	FUS-MS	FUS-MS
Client I.D.																			
RAM 1	50	2	<20	<10	<30	15	2	14	289	8	<2	<0.5	<0.2	5	1.4	6	8.5	17.1	2.17
RG 1	<20	<1	<20	<10	<30	13	1	<5	2	7	<2	<0.5	<0.2	5	1.3	<0.5	2.6	6.4	0.9
RG 5	40	2	<20	<10	<30	18	2	<5	291	11	<2	<0.5	<0.2	7	1.3	5.1	12.7	27.7	3.37
BG 1D	<20	<1	<20	<10	80	20	2	9	266	21	<2	<0.5	<0.2	2	1.9	10.3	57.6	104	12.4
BG 3	50	<1	<20	<10	40	19	2	14	275	18	<2	<0.5	<0.2	3	1.2	4.8	47.1	97.6	11.5
BG 5	<20	2	<20	<10	30	19	2	5	277	20	2	<0.5	<0.2	4	1.4	17.2	64.4	125	14.9
BG 2	40	<1	<20	<10	50	20	2	6	259	21	<2	<0.5	<0.2	5	1.6	4.3	43.9	101	10.4
Element:	Nd	Sm	Eu	Gd	Tb	Dy	Ho	Er	Tm	Yb	Lu	Hf	Ta	W	Tl	Pb	Bi	Th	U
Units:	ppm	ppm	ppm	ppm	ppm	ppm	ppm	ppm	ppm	ppm	ppm	ppm	ppm	ppm	ppm	ppm	ppm	ppm	ppm
Detection Limit:	0.1	0.1	0.05	0.1	0.1	0.1	0.1	0.1	0.05	0.1	0.04	0.2	0.1	1	0.1	5	0.4	0.1	0.1
Reference Method:	FUS-MS	FUS-MS	FUS-MS	FUS-MS	FUS-MS	FUS-MS	FUS-MS	FUS-MS	FUS-MS	FUS-MS	FUS-MS	FUS-MS	FUS-MS	FUS-MS	FUS-MS	FUS-MS	FUS-MS	FUS-MS	FUS-MS
Client I.D.																			
RAM 1	9.1	2.1	0.25	2.2	0.4	2.7	0.5	1.1	0.15	0.9	0.1	1.9	1.3	3	1.9	17	<0.4	5.4	2.5
RG 1	5	1.6	0.16	1.9	0.4	2.6	0.4	1.1	0.14	0.8	0.09	1.6	1	3	<0.1	<5	<0.4	4.8	1.4
RG 5	13.7	3.2	0.33	3.3	0.7	3.8	0.6	1.6	0.22	1.2	0.14	2.4	1.8	3	1.5	18	<0.4	8.1	4.6
BG 1D	42.1	7.3	1.13	6	1.1	6.3	1.3	4.2	0.67	4.2	0.61	6.2	1.8	2	1.5	37	<0.4	17.1	3.2
BG 3	41.1	9	0.73	8.7	1.6	9.2	1.8	5.5	0.84	5	0.71	6.2	1.5	1	1.6	37	<0.4	21.3	4.1
BG 5	52	10	1.14	8.5	1.5	8.8	1.8	5.6	0.85	5.3	0.74	7.4	1.9	1	1.3	31	<0.4	21.5	4.3
BG 2	37.3	8	1.07	7.7	1.4	8.8	1.8	5.6	0.86	5.3	0.76	6.9	1.8	2	1.7	27	<0.4	21	4.9

6. Conclusion

The concordia ages, geochemical signature and thin section microscopy lead to the following interpretation of the granite formation in the Harz Mountains: Between 290 and 270 Ma two processes in the southern part of the Rheno-Hercynian Zone of the Central European Variscides dominated: (i) Extension and thinning of the lithosphere caused the formation of the upper Rotliegend molasse basins, such as the Ilfelder Becken, Meisdorfer Becken and the Saalesenke; and (ii) The epirogenetic shear stress leads to a doming in the asthenosphere. That effects the intrusion of a fluidal phase of mantle magma and a partial anaxsis of the lithospheric rock. Massiv plutons intruded along the subduction zone as linear belts and crystallized with a mineral admixture composition of asthenospheric and lithospheric elements. The Brocken granite crystallized under an asthenospheric-lithospheric mixed petrochemical and petrophysical milieu with a geochemical signature of a primitive mantle rock. The Ramberg granite crystallized in the upper crust under lithospheric conditions. The geochemical signature of the Brocken granite reflects an element compositions of the asthenosphere, like enrichment in heavy metals and REE. The Ramberg granite corresponds with lithospheric rocks by having high concentration on SiO₂, light metals and trace elements and a lower concentration of REE. The zircon types of both granites support those results. The dominating zircon shapes D, P5 and S25 of the Brocken granite samples imply temperature conditions between 800–900 °C during crystallization. The Ramberg granite zircons crystallized as G1 and P1 types between 600 and 650 °C. Hence the intrusion and crystallization of the granite was cogenetic but in different levels in the lithosphere and under different geochemical conditions. The epirogenetic shear stress caused fissures, in which magma intruded and crystallized fine-grained. The typical volcanic lodes, like the “Mittelharzer Gänge” or the Bodegang evolved. Tietz (1996) documented the zircons of the granitoid-xenolith from the “Bodegang” and suggested a petrographical relation between those and the zircons of the Ramberg granite. This could be verified with the dominating zircon types G1 and P in both geological complexes. Additionally Tietz identified the zircon types P3 and P4 for the Brocken granite, which is also in good agreement with our results. The equal crystallisation age of the needle-shaped zircons of the Brocken 283.0 ± 2.1 Ma and of the Ramberg I) 283.0 ± 2.8 Ma, and ad-

ditionally the described geological conditions during the upper Rotliegend (Lower Permian) suggest a cogenetic geotectonic origin in the shear stresses and a cogenetic intrusion. Therefore our results are in good agreement with previous results (Benek 1965; Schoell et al. 1973; Wachendorf and Krebs 1974; Baumann et al. 1991; Mohr 1993; Tietz 1996) assigning the intrusion after the variscian orogeny to the upper Rotliegend. A second, earlier crystallization phase of the Ramberg granite was already proposed by Eidam and Seim (1971) and could now be dated to 289.3 ± 0.59 Ma.

Acknowledgement

We thank Dr. K. Drost for help with the mineral separations and preparation of the thin sections.

References

- Baumann, A. et al (1991): Isotopic age determinations of crystalline rocks of the Upper Harz Mountains, Germany. *International Journal of Earth Science* **80**(3):669–690
- Benek, R (1965): Die Form des Ramberg-Granitkörpers im Harz. *Monatsberichte der deutschen Akademie der Wissenschaften zu Berlin* **7**, Berlin: 823–826.
- Eidam, J., Seim, R. (1971): Zur Geochemie und Genese des Rambergmassivs (Harz). *Chemie der Erde* **29**, Jena: 277–333
- Feldmann, L. et al. (2002): Die geologische Entwicklung der Tiefebene und der Mittelgebirge in Niedersachsen. *Veröffentlichungen der Akademie für Geowissenschaften Hannover e. V.*: 9–13.
- Geisler-Wierwille, T. (1999): U-Th-Gesamtblei-Datierung von Zirkonen mit Hilfe der Elektronenstrahl-Mikrosonde Methodik und Anwendungsbeispiele. *Dissertation, Hamburg.*
- Jeffries, T. et al. (2003): Advances in U-Pb geochronology using a frequency quintupled Nd YAG based laser ablation system ($\lambda = 213$ nm) and quadrupole based ICP-MS. *J Anal At Spectrom* **18**: 847–855.
- Linnemann, U., Romer, R. L. (2002): The Cadomian Orogeny in Saxo-Thuringia, Germany geochemical and Nd-Sr-Pb isotopic characterization of marginal basins with constraints to geotectonic setting and provenance. *Tectonophysics* **352**: 33–64.
- Ludwig, K. R. (1998) Calculation of uncertainties of U-Pb isotope data. *Earth and Planetary Science letters* **46**: 212–220.

- Ludwig, K. R. (2001): Users manual for isoplot/Ex Version 249. A Geochronological Toolkit for Microsoft Excel Berkeley Geochronology Center. Special Publication No 1a, Berkeley.
- Markl, G. (2004) Minerale und Gesteine – Eigenschaften, Bildung, Untersuchung. Elsevier, München.
- Mohr, K. (1993) Geologie und Minerallagerstätten des Harzes. 2nd edn. Stuttgart.
- Pearce, J. A., Harris, N. B. W., Tindle, A. G (1984): Trace Element Discrimination Diagrams for the Tectonic Interpretation of Granitic Rocks. *Journal of Petrology* **25** (4): 956–983.
- Seim, R. (1963): Petrologische Untersuchungen an kontaktmetasomatischen Gesteinen am Ostrand des Brockenmassivs (Harz). *Geologie* **37**: 66.
- Seim, R, Eidam, J. (1974): Vergleichende geochemische Untersuchung der Granite des Brocken- und Rambergmassivs im Harz. *Chemie der Erde* **33**: 31 –46.
- Steiger, R. H., Jäger, E. (1977): Subcommittee on geochronology Convention on the use of decay constants in Geo- and Cosmo chronology. *Earth and Planetary Science Letters* **36** (3): 359 – 362.
- Tietz, O. (1996): Zur Geologie, Geochemie, Zirkon- und Xenolithführung des Bodegangs an den Gewitterklippen bei Thale (Harz), sowie vergleichende Untersuchungen zur Zirkontypologie benachbarter permosilesicher Magmatite. *Abhandlungen und Berichte des Naturkundemuseums Görlitz*, **69** (4): 1 – 100.
- Wachendorf, H. (1986): Der Harz. *Geologisches Jahrbuch A* 91 (89), Hannover.
- Wachendorf, H. (2002): Harz prävariszische und variszische Prozesse. Programm und Kurzfassungen der Vorträge Arbeitstreffen Harzgeologie 2002: 1–3.